Supporting information:

High-Temperature Thin Flexible Transparent Ni-based Heater Patterned by Laser-Induced Reductive Sintering on Colorless Polyimide

Vu Binh Nam[1], Jaeho Shin[2], Ahyoung Choi[3], Hoimyung Choi[1], Seung Hwan Ko[2], and Daeho Lee[1]*

[1]Department of Mechanical Engineering, Gachon University, 1342 Seongnamdaero, Sujeong-gu, Seongnam, Gyeonggi 13120, South Korea

[2]Department of Mechanical Engineering, Seoul National University, 1 Gwanak-ro, Gwanak-gu, Seoul 08826, South Korea

[3]Department of Software, Gachon University, 1342 Seongnamdaero, Sujeong-gu, Seongnam, Gyeonggi 13120, South Korea

*E-mail: dhl@gachon.ac.kr

*Tel.: +82-31-750-5518

1.The uniform NiO_x thin film on colorless polyimide

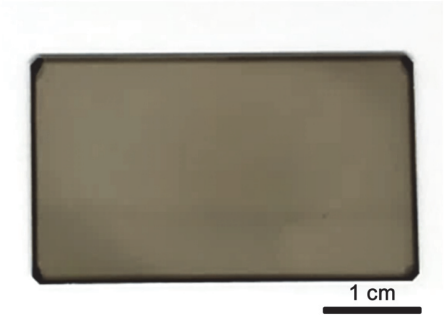

Fig. S1. A uniform spin-coated (1000 rpm for 60 s) NiO_x thin film on a colorless polyimide (cPI) film formed on a glass substrate.

2.The scale-up reaction for producing NiO_x nanoparticle ink.

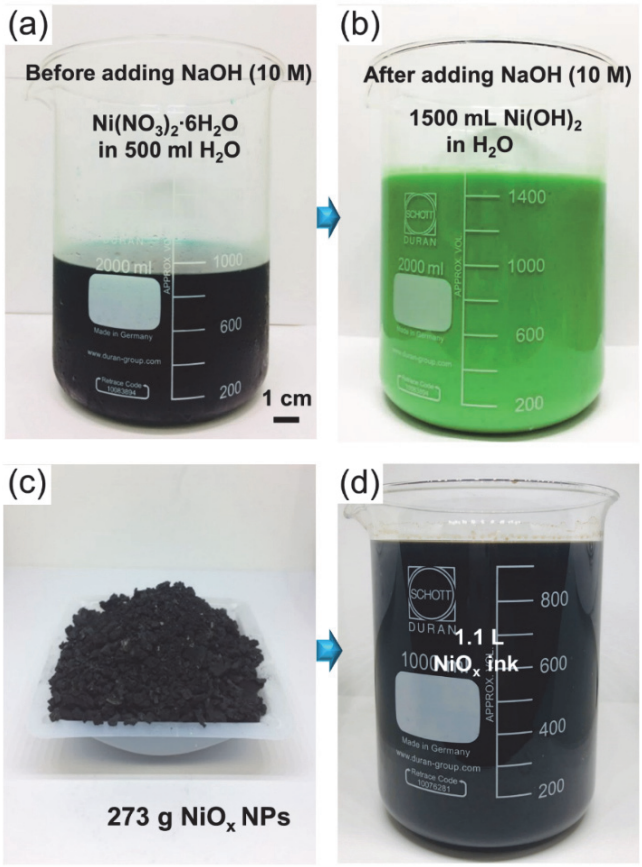

Fig. S2. A scale-up reaction: (a) $Ni(NO_3)_2 \cdot 6H_2O$ (2.5 mol) is easily dispersed in deionized water (500 mL). (b) The pH value of solution was accurately controlled to 10 by adding NaOH solution (10 M). (c) 273 g of NiO_x nanoparticle (NPs) after calcination at 270 °C for 2 h. (d) 1.1 L of NiO_x NP ink containing NiO_x NPs (23.8 wt%), PVP (5.2 wt%), CTAB (0.4 wt%), and 1-pentanol (70.6 wt%).

3. Characterizations of NiO_x nanoparticles

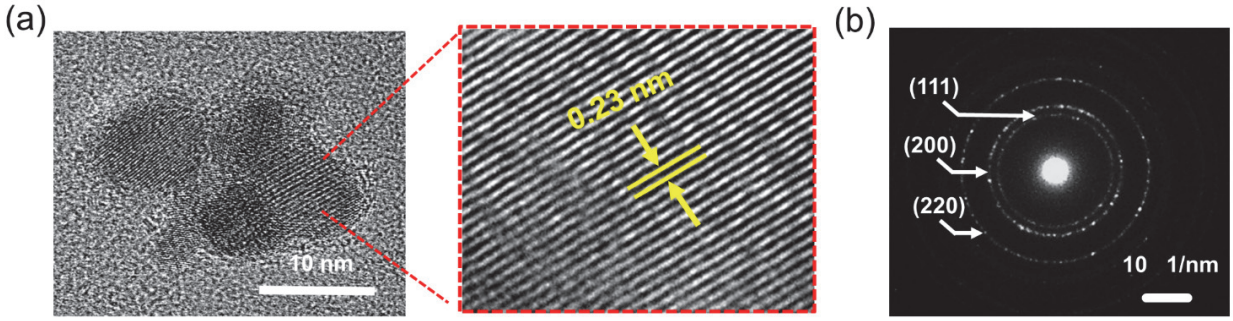

Fig. S3. (a) High-resolution transmission electron microscopy image of NiO_x nanoparticle (NPs). (b) The electron diffraction pattern from NiO_x NPs. NiO_x NPs have a face-centered cubic (FCC) crystalline structure with the space between two adjacent fringes of 0.23 nm, corresponding to the (111) plane.

4.Laser-induced reductive sintering setup

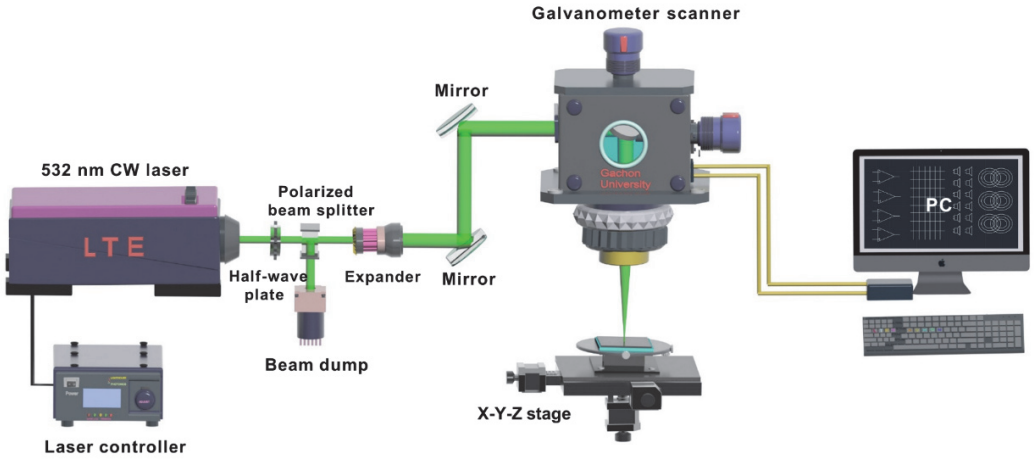

Fig. S4. Schematic illustration of the laser-induced reductive sintering (LRS) setup.

5. The photographic image of arbitrary Ni patterns marked on colorless polyimide

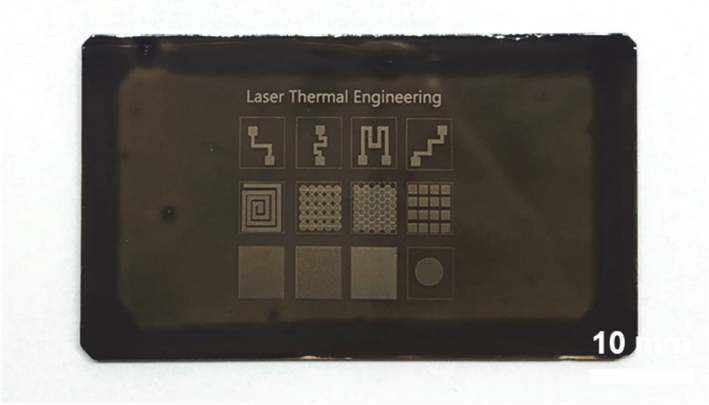

Fig. S5. A photographic image of arbitrary Ni patterns marked on colorless polyimide (cPI) before washing.

6. The uniformity of the Ni/cPI heating profile

As shown in **Fig. S6**, the central part of the heater shows an even temperature profile. The analysis revealed that most of the calculated standard deviations were found to be due to the relatively low temperature observed at the boundary of the heater. This indicates that even a considerable portion of the 5.2% of temperature irregularity could be attributable to the heat dissipation to the surrounding area, which is a natural, unavoidable result. In particular, since the temperature deviation at the boundary of the heater can be expected to be larger as the temperature at the center of the heater high as in this study, the temperature deviation originated from the limit of the heater itself can be expected to be smaller in practice.

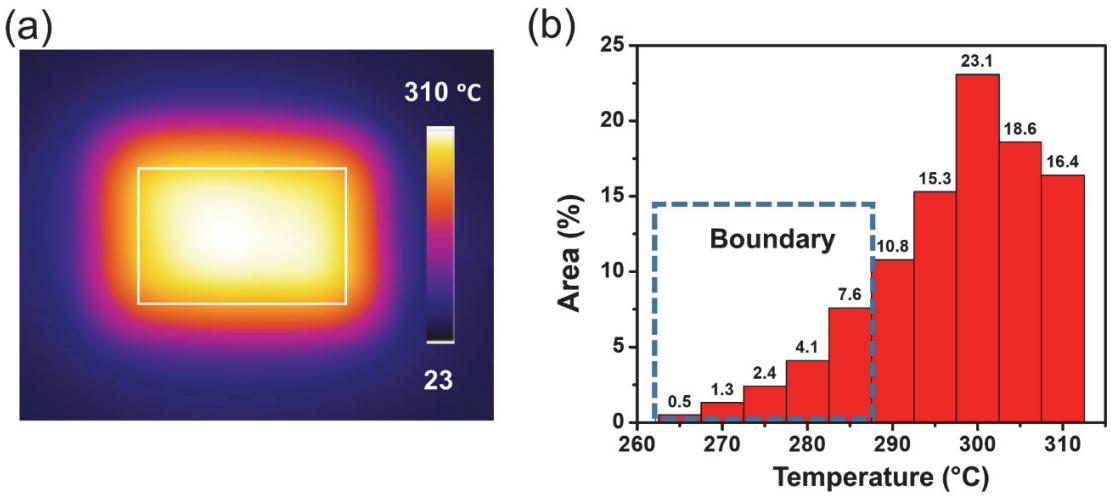

Fig. S6. Uniformity of the Ni/cPI heating profile. (a) Infrared (IR) image of the heater and (b) the corresponding temperature profile of the heater area.

7. The performance of the heater under bending condition and its failure mechanics.

In the experiment, the Ni/cPI heater was bent gradually to a smaller radius of curvature, while the DC voltage was supplied continuously. As can be seen from the IR image of **Fig. S7a**, the heating characteristics of the heater did not show appreciable changes even under substantial bending at a radius of 2 mm, and no signs of failure such as hot-spot were observed. However, as shown in **Fig. S7b**, under the bending condition of 1 mm radius, the heater showed sudden mechanical failure, and this phenomenon was reproduced with the 5 samples. As a result of microscopic observation, it was confirmed that such sudden mechanical failure was not accompanied by delamination on the Ni and cPI substrates. In addition, considering that no abnormality was observed in the heating characteristics of the heater until just before fracture, it seems that the mechanical failure was caused by the mechanical failure of the cPI substrate rather than a compromised mechanical integrity between the Ni and cPI substrate. Furthermore, since the substrate's mechanical failure is regarded as a limitation of the lab-prepared cPI, it is expected that the mechanical robustness of the Ni/cPI heater could be enhanced by using a commercially available cPI substrate in the future.

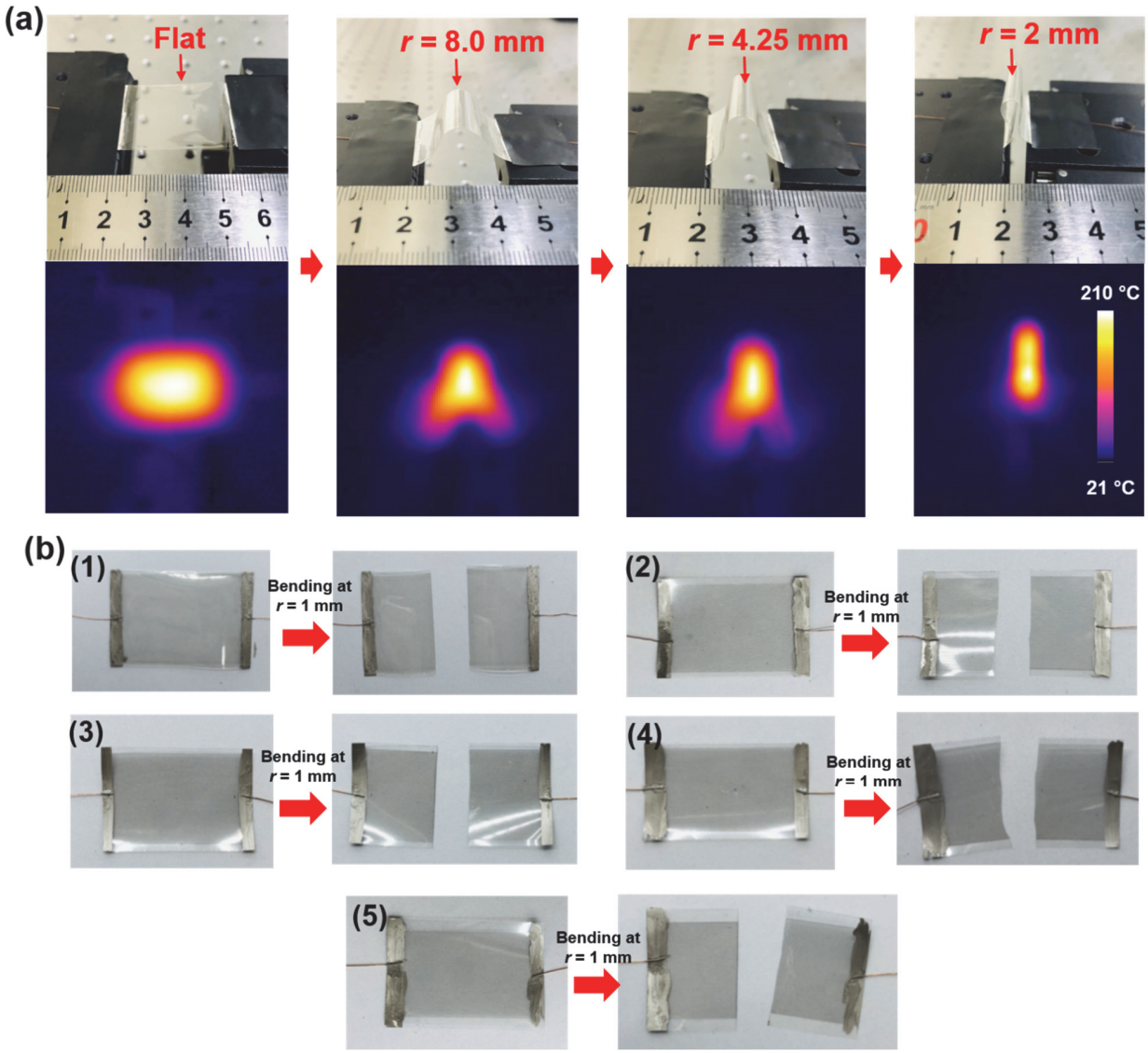

Fig. S7. Heater performance under mechanical stress. (a) Digital and infrared (IR) images of the heater at various bending radii. (b) Photographic images of 5 heaters before and after bending radius of 1 mm.

8. The sufficient number of tested samples

One of the major advantages of the laser process introduced here is its highly simplified process. Compared to the conventional vacuum deposition and etching process, the laser digital patterning method comprising only four steps: spin coating and drying of nanoparticle inks, laser irradiation, and cleaning, allows the high level of manufacturing repeatability by significantly lowering the chance of the random events. As a result, the simplified fabrication process realizes the minimal batch-to-batch variation. To support this, we present the digital and IR images of 10 different heaters with the same design, which were fabricated and evaluated for this study (**Fig. S8**). The experimental result presented in the original manuscript was a representative result from these devices.

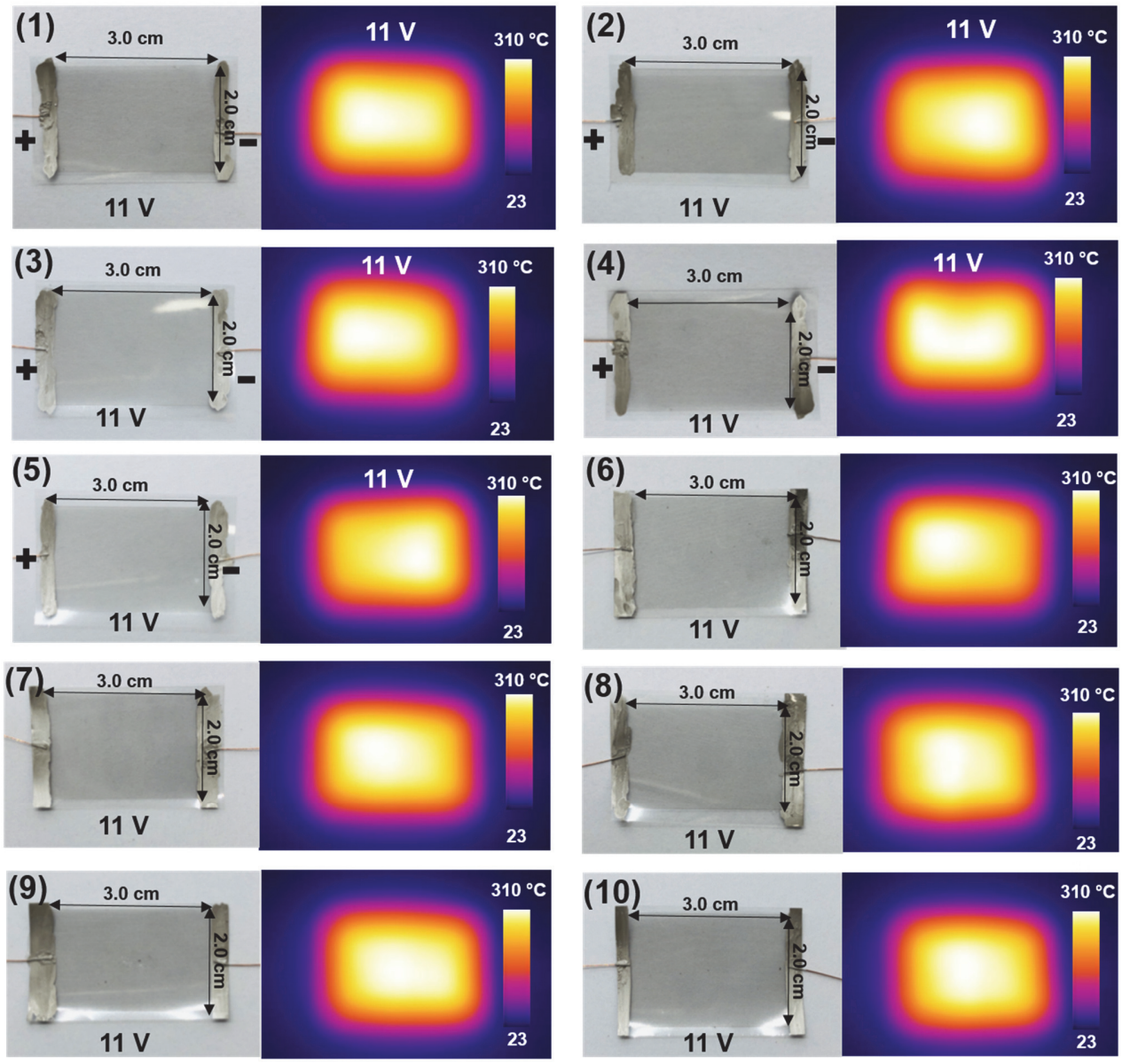

Fig. S8. Photographic images and infrared (IR) images of 10 Ni/cPI heaters under applying the DC voltage of 11 V.

9. The non-uniform distribution of heat of the heater exceeding 310 °C

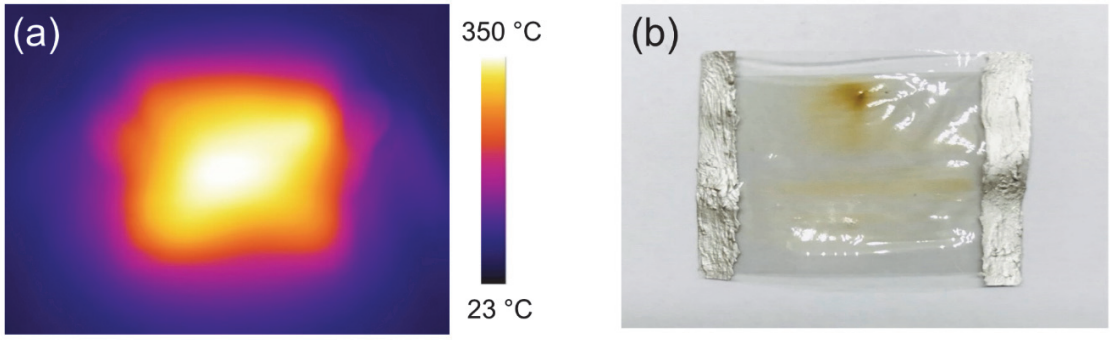

Fig. S9. Infrared (IR) image of a flexible transparent Ni-grid heater on colorless polyimide (cPI) (a) and its photo-image (b) at heating temperature exceeding 310 °C.

10. Discussion on the tape-pull test

The need for a standardized test is something that we were also aware of from the preparation stage. However, we would like to note that there have been limitations in applying the existing standardized peeling test technique to this study. Most of the existing standardized peeling test techniques have been developed suitable for testing the adhesion between hard substrates and thin films. On the other hand, the transparent heater developed in this study uses a very thin (~25 μm), flexible substrate for its research purposes. Therefore, during the peeling test using high-adhesive tape, there was a limit that the substrate was damaged first. In the background, where a simplified test using 3M magic tape was included in the previous text, there were limitations in this measurement. In many existing studies [1-3], we found that the peeling tests were performed using 3M Scotch 610 tape, which has higher adhesion strength than 3M magic tape, and it seems that the tape is also partially applied to the industry standard D3359. Based on this finding, a peeling test was performed using 3M Scotch 610 tape, and the results were shown in **Fig. 5e**.

11. The ultrasonication test

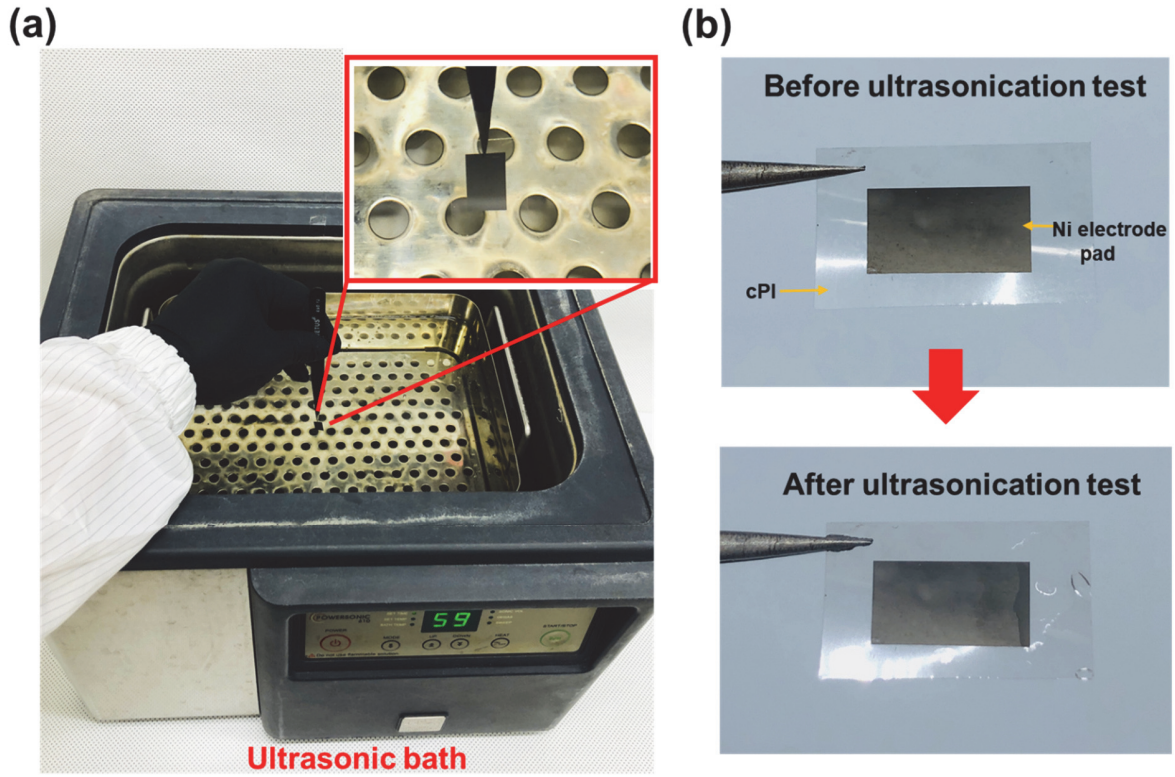

Fig. S11. (a) Photographic images of the ultrasonication test by immersing the Ni electrode pad on colorless polyimide (cPI) in the ultrasonic bath. (b) The Ni electrode pad before and after the test.

Video S1. Ultra-thin colorless polyimide (cPI)

Video S2. Fast heating and cooling rates of the flexible transparent Ni-based heater

Video S3. Thermal durability of the Ni-based heater at 310 °C for 5 min

Video S4. Boiling water using the flexible transparent Ni-based heater

Video S5. Ice (15 mm × 15 mm × 5 mm, 1.3g) melting comparison at different temperatures of the heater

Video S6. Tape-pull test of the Ni electrodes on the cPI substrate

Video S7. Ultrasonication test of the Ni electrodes on the cPI substrate

References

1. S. J. Park, T.-J. Ko, J. Yoon, M.-W. Moon, K. H. Oh and J. H. Han, *Applied Surface Science*, 2018, **427**, 1-9.
2. Y. Sun, C. Du, M. Wu, L. Zhao, S. Yu, B. Gong and Q. Ding, *Nanotechnology*, 2020, **31**, 375303.
3. G. J. Han, S. You, H. W. Choi and K. H. Kim, *Molecular Crystals and Liquid Crystals*, 2017, **645**, 255-260.